Optimal Operation of PV-integrated Reconfigurable Microgrids and Computational Burden

Author(s): Zandrazavi, Seyed Farhad; Shafie-Khah, Miadreza

Title: Optimal Operation of PV-integrated Reconfigurable Microgrids and Computational Burden

Year: 2024

Version: Accepted manuscript

Please cite the original version:

Zandrazavi, S. F., & Shafie-Khah, M. (2024). Optimal Operation of PV-integrated Reconfigurable Microgrids and Computational Burden. In *2024 IEEE International Conference on Environment and Electrical Engineering and 2024 IEEE Industrial and Commercial Power Systems Europe (EEEIC / I&CPS Europe)*. IEEE. https://doi.org/10.1109/EEEIC/ICPSEurope61470.2024.10750960

Optimal Operation of PV-integrated Reconfigurable Microgrids and Computational Burden

Seyed Farhad Zandrazavi
School of Technology and Innovations
University of Vaasa
Vaasa, Finland
seyed.zandrazavi@uwasa.fi

Miadreza Shafie-khah
School of Technology and Innovations
University of Vaasa
Vaasa, Finland
mshafiek@uwasa.fi

***Abstract*—This paper addresses the significant potential of reconfiguration in renewable-based microgrids (MGs), emphasizing not only its practical benefits but also the computational challenges involved. Firstly, a nonlinear non-convex model developed for the optimal operation of photovoltaic (PV)-integrated reconfigurable microgrids (RMGs). To guarantee the optimality of the solutions, we further refine the model by extracting a mixed-integer linear programming model, achieved through the implementation of piecewise linearization technique and approximation. To substantiate the efficacy and importance of reconfiguration in MGs, comparative analyses of two distinct case studies—one with reconfiguration and one without are presented. These comparisons not only highlight the operational improvements afforded by reconfiguration but also shed light on the computational complexities encountered. Moreover, the impact of different radiality method selections on the computational time is explored. Our findings validate the significant role of reconfiguration in enhancing the performance of renewable-based MGs while also emphasizing the critical consideration of computational burden in the design and implementation of such systems.**

Keywords— Computational burden, optimal operation, photovoltaic, radiality, reconfigurable microgrid.

NOMENCLATURE

Acronyms

DG	Distributed generation
DN	Distribution network
DR	Demand response
EU	European Union
EV	Electric vehicle
GHG	Greenhouse gas
MILP	Mixed-integer linear programming
OF	Objective function
PL	Power loss
PV	Photovoltaic
RMG	Reconfigurable microgrid
RPF	Reverse power flow
TVAC-PSO	Time-varying acceleration coefficients particle swarm optimization

Sets & Indices

L	Set for lines
dg	Index for DG
i, j, k	Index for bus
ij	Index for line
t	Index for time interval
ω	Index for pieces in piecewise linearization

This research has received funding from the European Union's Horizon 2020 research and innovation programme, within the OpenInnoTrain project under the Marie Skłodowska-Curie grant agreement no. 823971. The content of this publication does not reflect the official opinion of the European Union. Responsibility for the information and views expressed in this publication lies entirely with the authors. Seyed Farhad Zandrazavi also acknowledges Finnish Cultural Foundation for grant 00241288 Central Fund.

Parameters

$\mathbb{C}_t^{Main}$	Cost of buying energy from main grid
$\mathbb{C}_{dg}^a, \mathbb{C}_{dg}^b, \mathbb{C}_{dg}^c$	Coefficients of DG cost
$E_{bs}^{min}, E_{bs}^{max}$	Minimum and maximum energy level of battery
$\check{E}_{bs}^{BS}$	Initial energy level of battery
$\eta_{bs}^{BS}, \beta_{bs}^{BS}$	Efficiency & Self-discharge rate of battery
$P_{pv,t}^{ava}$	Available power for PV units
R_{ij}, X_{ij}, Z_{ij}	Resistance, reactance, & impedance of lines
$L_{i,t}^P, L_{i,t}^P$	Active & reactive power demand
V_i^{est}	Estimated voltage
I_{ij}^{max}	Maximum current
$P_{dg}^{min}, P_{dg}^{max}$	Minimum & maximum generation of DG
f_{dg}^{DG}	Power factor of DG
V^{min}, V^{max}	Minimum & maximum voltage
$M_{ij,\omega}^{PQ}$	Slope in linearization of power flowing in line
$M_{dg,\omega}^{DG}$	Slope in linearization of DG's power
Δ_t	Hourly time intervals
ΔQ_{ij}^{max}	Maximum discretization blocks of reactive power
ΔP_{ij}^{max}	Maximum discretization blocks of active power
ΔP_{dg}^{max}	Maximum discretization blocks of DG's power
$\overline{\omega}$	Number of pieces in piecewise linearization

Variables

$\varrho_{dg,t}^{DG}$	Binary variable to model the commitment of DG
$\Gamma_{ij,t}$	Auxiliary variable related to reconfiguration
$p_{i,t}^{Main}, q_{i,t}^{Main}$	Active & reactive power imported from the main grid
$e_{bs,t}^{BS}$	Energy level of battery
$p_{bs,t}^{BS}$	Active power of battery
$p_{bs,t}^{BS+}, p_{bs,t}^{BS-}$	Charging/discharging power of battery
$p_{dg,t}^{DG}, q_{dg,t}^{DG}$	Active & reactive power of DG
$P_{pv,t}^{ava}$	Available solar power
$p_{pv,t}^{PV}$	Active power of PV
$p_{ij,t}, q_{ij,t}$	Active & reactive power flowing in lines
$v_{i,t}, i_{ij,t}$	Voltage & current
v_i^{sqr}, i_{ij}^{sqr}	Square of voltage & current
$\Delta p_{ij,\omega}, \Delta q_{ij,\omega}$	Discretization blocks of power flowing in line
$p_{bn,t}^+, q_{bn,t}^+$	Active & reactive power in lines (positive direction)
$p_{bn,t}^-, q_{bn,t}^-$	Active & reactive power in lines (negative direction)
$y_{ij,t}^+, y_{ij,t}^-$	Binary variable associated with status of switches

I. INTRODUCTION

The European Union (EU)'s ambitious goal to enhance its greenhouse gas (GHG) emissions reduction target from 40% to 55% by 2030, paving the way for Europe to become the first climate-neutral continent by 2050 [1]. Focused on the crucial role of photovoltaics (PV) in this transition, the 55% GHG reduction necessitates expanding the cumulative PV capacity in the EU and the United Kingdom by approximately 33% [1]. To this end, microgrids (MGs) can play a decisive role by accommodating more PV units in the distribution level. PV-powered MGs are increasingly favored worldwide due to their utilization of globally available solar energy, supported by cost-effective and reliable technology [2]. Furthermore, they are bolstered by encouraging policies and incentives, making them suitable for a variety of applications such as industry, education, small communities, residential rooftops, and water pumping for irrigation and community use [2].

A. Motivation

The production of electricity via PV systems is characterized by inherent intermittency, which does not consistently match with periods of elevated demand for electricity. Consequently, the integration of PV units into MGs can cause a condition known as reverse power flow (RPF). RPF can result in elevated voltage levels and the potential for contingency issues. Therefore, the amount of power that PV units are permitted to inject into the grid is subject to limitations, necessitating the curtailment of PV generation to mitigate these concerns [3]. However, reconfiguration has considered in the literature as a promising method not only to reduce the PV curtailment [4] but also to improve voltage profile and reduce the power loss (PL) [5].

B. Literature review

Some of the previous works focus on using metaheuristic algorithms to solve optimal operation of reconfigurable microgrids (RMGs). In [6], a framework for day-ahead optimal scheduling RMGs, with an emphasis on minimizing PL, is presented. The developed optimization model is solved using a hybrid metaheuristic optimization approach to determine efficient and optimal network reconfiguration as well as scheduling of distributed generation (DG) units. Time-varying acceleration coefficients particle swarm optimization (TVAC-PSO) algorithm is used in [7] to solve the optimal operation of RMG considering different DG units and energy storages to maximize the profit of MGs. Similarly, in [8], TVAC-PSO is utilized to solve a risk-based optimal operation of RMG, while uncertainties linked to renewable energy and electricity prices are included. In [9], authors show that not only RMGs can improve the incorporation of plug-in electric vehicles (EVs) into the power grid but also can minimize operational cost and enhance the reliability of MGs. A modified clonal selection algorithm is presented to solve the proposed model [9]. Despite the valuable contributions and findings of these studies, the optimality of solutions, and tuning and randomness of the metaheuristic algorithms are still problematic. On the other hand, there are other previous studies in which instead of metaheuristic algorithms, exact mathematical models are extracted and solved by off-shelf commercial solvers. A mixed-integer second-order cone programming model is developed in [10] to minimize the cost of MGs, while EVs and demand response (DR) are considered. Probabilistic power flow for wind-power-integrated RMG is developed in [11] and solved by using CPLEX [12], while a clustering approach is used to reduce the number of samples compared to the Monte Carlo simulation. Although previous studies have made important contributions, they have not tackled the computational complexity involved in determining the optimal operation of RMG through precise mathematical modeling.

C. Contribution

As previously mentioned, reconfiguration can yield numerous practical advantages for renewable-based MGs. However, it remains important to also consider the issues from a computational perspective. In conclusion, the key contributions of this paper are outlined as follow:

- Developing a nonlinear model for optimal operation of PV-integrated reconfigurable microgrids
- Extracting the mixed-integer linear programming model (MILP) by utilizing piecewise linearization to ensure optimality of solutions
- Validating the importance of reconfiguration in microgrids by comparing two case studies with and without reconfiguration
- Validating the computational burden of the proposed model as well as influence of radiality method selection on computational time

II. Optimization Model

In this section, a nonlinear nonconvex model for the optimal day-ahead scheduling of PV-integrated RMG considering different methods for including radiality, is presented. After that, the model is linearized using piecewise linearization approach to extract the respective MILP model.

A. Nonlinear Nonconvex Model of the Optimal Operation of RMG

In (1), the nonlinear objective function (OF), which is the operational cost minimization, is presented. This OF includes two terms, where the first term is associated with the cost of purchasing the power from the main grid, while the second term is corresponded to the generation and scheduling of DG units.

$$min\left(\begin{array}{c}\sum_{t}\Delta_t\mathbb{C}_t^{Main}p_t^{Main}\\ +\sum_{dg}\sum_{t}\mathbb{C}_{dg}^{a}\varrho_{dg,t}^{DG}+\Delta_t p_{dg,t}^{DG}\mathbb{C}_{dg}^{b}+\left(\Delta_t p_{dg,t}^{DG}\right)^2\mathbb{C}_{dg}^{c}\end{array}\right) \tag{1}$$

Equations (2)–(5) introduce a bidirectional nonlinear nonconvex AC power flow formula as referenced in [13]. The active and reactive power balances are detailed in the first two equations. In addition, equations (4) and (5) model the relationship among voltage, current, and power in RMGs. In (6), the proper limit for auxiliary variable $\Gamma_{ij,t}$ is considered which is either zero or the maximum possible voltage rise/drop in the system. Constraints (7) and (8) ensure that voltages and currents of the RMG remain in the permissible ranges to avoid any technical problems. To include the both positive and negative directions of the active and reactive power flowing in the lines, equations (9) and (10) are included in the model. Suitable limits on these directional power flows are considered in (11)–(14) in accordance with the status of switches. As aforementioned, the generation of renewable resources may result to RPF and technical issues; hence through constraint (15), the plausibility of renewable curtailment is considered. Technical limitations of DG units are presented in (16)–(19), where upper and lower bounds for active and reactive power generations are determined. Battery charging/discharging model and limits are presented in (20)–(26) [14]. In (20)–(22), the charging ($P_{bs,t}^{BS+}$) and discharging ($p_{bs,t}^{BS-}$) is defined and respective limits are presented. Constraint (23) ensures that charging and discharging cannot happen simultaneously. The relationship between power and energy level of batteries is modeled in (24) and (25). The constraint (26) determines the upper and lower bounds for the batteries to guarantee the desirable lifespans for batteries.

$$\sum_{ki|ki\in L} p_{ki,t} - \sum_{ij|ij\in L}\left(p_{ij,t} + R_{ij} i_{ij,t}^2\right) + \sum_{i|b_{sub=i}} p_{i,t}^{Main} + \sum_{dg|b_{dg}=i} p_{dg,t}^{DG} + \sum_{pv|b_{pv}=i} p_{pv,t}^{PV} = L_{i,t}^{P} + \sum_{bs|b_{bs}=i} p_{bs,t}^{BS};\ \forall i,t \tag{2}$$

$$\sum_{ki|ki\in L} q_{ki,t} - \sum_{ij|ij\in L}\left(q_{ij,t} + X_{ij} i_{ij,t}^2\right) + \sum_{i|i=b_{sub}} q_{i,t}^{Main} + \sum_{dg|b_{dg}=i} q_{dg,t}^{DG} = L_{i,t}^{Q};\ \forall i,t \tag{3}$$

$$v_{i,t}^2 - v_{j,t}^2 = 2\left(R_{ij}p_{ij,t} + X_{ij}q_{ij,t}\right) + Z_{ij}^2 i_{ij,t}^2 + \Gamma_{ij,t};\ \forall ij|ij\in L,t \tag{4}$$

$$v_{i,t}^2 i_{ij,t}^2 \geq \left(p_{ij,t}^2 + q_{ij,t}^2\right);\ \forall ij|ij\in L,t \tag{5}$$

$$-((V^{max})^2 - (V^{min})^2)\left(1 - \left(y_{ij,t}^+ + y_{ij,t}^-\right)\right) \leq \Gamma_{ij,t} \leq ((V^{max})^2 - (V^{min})^2)\left(1 - \left(y_{ij,t}^+ + y_{ij,t}^-\right)\right);\ \forall ij|ij\in L,t \tag{6}$$

$$(V^{min})^2 \leq v_{i,t}^2 \leq (V^{max})^2;\ \forall i,t \tag{7}$$

$$0 \leq i_{ij,t}^2 \leq \left(I_{ij}^{max}\right)^2\left(y_{ij}^+ + y_{ij}^-\right);\ \forall ij|ij\in L,t \tag{8}$$

$$p_{ij,t} = p_{ij,t}^+ - p_{ij,t}^-;\ \forall ij|ij\in L,t \tag{9}$$

$$q_{ij,t} = q_{ij,t}^+ - q_{ij,t}^-;\ \forall ij|ij\in L,t \tag{10}$$

$$0 \leq p_{ij,t}^+ \leq V^{max} I_{ij}^{max} y_{ij,t}^+;\ \forall ij|ij\in L,t \tag{11}$$

$$0 \leq p_{ij,t}^- \leq V^{max} I_{ij}^{max} y_{ij,t}^-;\ \forall ij|ij\in L,t \tag{12}$$

$$0 \leq q_{ij,t}^+ \leq V^{max} I_{ij}^{max} y_{ij,t}^+;\ \forall ij|ij\in L,t \tag{13}$$

$$0 \leq q_{ij,t}^- \leq V^{max} I_{ij}^{max} y_{ij,t}^-;\ \forall ij|ij\in L,t \tag{14}$$

$$0 \leq p_{pv,t}^{PV} \leq P_{pv,t}^{ava} \tag{15}$$

$$p_{dg,t}^{DG} \geq \varrho_{dg,t}^{DG} P_{dg}^{min};\ \forall dg,t \tag{16}$$

$$p_{dg,t}^{DG} \leq \varrho_{dg,t}^{DG} P_{dg}^{max};\ \forall dg,t \tag{17}$$

$$q_{dg,t}^{DG} \leq p_{dg,t}^{DG}\, tan\left(cos^{-1}\left(f_{dg}^{DG}\right)\right);\ \forall dg,t \tag{18}$$

$$q_{dg,t}^{DG} \geq -p_{dg,t}^{DG}\, tan\left(cos^{-1}\left(f_{dg}^{DG}\right)\right);\ \forall dg,t \tag{19}$$

$$0 \leq P_{bs,t}^{BS+} \leq P_{bs}^{max} \varrho_{bs,t}^{+};\ \forall bs,t \tag{20}$$

$$0 \leq P_{bs,t}^{BS-} \leq P_{dg}^{max} \varrho_{bs,t}^{-};\ \forall bs,t \tag{21}$$

$$p_{bs,t}^{BS} = p_{bs,t}^{BS+} - p_{bs,t}^{BS-};\ \forall bs,t \tag{22}$$

$$\varrho_{bs,t}^{+} + \varrho_{bs,t}^{-} \leq 1;\ \forall bs,t \tag{23}$$

$$e_{bs,t}^{BS} = \check{E}_{bs}^{BS} + \Delta_t\left(p_{bs,t}^{BS+}\eta_{bs}^{BS} - \frac{p_{bs,t,s}^{BS-}}{\eta_{bs}^{BS}} - e_{bs,t}^{BS}\beta_{bs}^{BS}\right);\forall bs,t|t=1 \tag{24}$$

$$e_{bs,t}^{BS} = e_{bs,t-1}^{BS} + \Delta_t\left(P_{bs,t}^{BS+}\eta_{bs}^{BS} - \frac{P_{bs,t,s}^{BS-}}{\eta_{bs}^{BS}} - e_{bs,t}^{BS}\beta_{bs}^{BS}\right);\ \forall bs,t|t\geq 1 \tag{25}$$

$$E_{bs}^{min} \leq e_{bs,t}^{BS} \leq E_{bs}^{max};\ \forall bs,t \tag{26}$$

B. Radiality Modeling

In the literature, there are different methods available to impose the radiality in DNs and MGs. For example, in [15] by considering similarity between radial topology of an DN with a tree in the graph theory a method for enforcing radiality is proposed. Accordingly, the configuration of a DN or MG, comprising Ψ_L buses, is considered radial if the count of closed switches is consistently one fewer than the overall number of buses, as indicated in (27). Binary variables $y_{ij,t}^+$ and $y_{ij,t}^-$ are defined to model the status of switches and cannot be one simultaneously as presented in (28).

$$\sum_{ij|ij\in L}\left(y_{ij,t}^+ + y_{ij,t}^-\right) = \Psi_L - 1;\ \forall t \tag{27}$$

$$y_{ij,t}^+ + y_{ij,t}^- \leq 1;\ \forall ij|ij\in L,t \tag{28}$$

In addition to the aforementioned method, another approach has been proposed in [16] to impose the radiality condition via parent bus-child bus path as presented in (28)–(30). The criteria for network radiality stem from a key feature of the spanning tree: each bus, with the exception of the root (substation bus), possesses precisely one parent. This feature can be modeled as presented in (29) and (30).

$$\sum_{j|(ij)\in L}\left(y_{ij,t}^-\right) + \sum_{j|(ji)\in L}\left(y_{ji,t}^+\right) = 1;\ \forall i>1,t \tag{29}$$

$$\sum_{j|(ij)\in L}\left(y_{ij,t}^-\right) + \sum_{j|(ji)\in L}\left(y_{ji,t}^+\right) = 0;\ \forall i=1,t \tag{30}$$

It is noteworthy that both models serve the same purpose: they aim to maintain the radial structure of the RMG or reconfigurable distribution networks. Therefore, solutions to the problem should not be influenced by the specific method used to model radiality. Nevertheless, comparing these two approaches show that the latter method include more constraints compared to the former approach as in addition to each time interval, constraint should be satisfied for each bus as well.

C. Linearization Procedure

The developed model, adept at nonlinear and nonconvex modeling, accurately captures the power flow and optimal operations within RMG. However, it does not ensure the optimality of its solutions. Consequently, this subsection outlines the process of linearizing the nonlinear model to address this limitation. OF presented in (1) as well as constraints (2)–(8) (except for (6), which is linear) are linearized. More details about this linearization approach can be found in [17]. Thus, (1) can be replaced by (31)–(33). where ΔP_{dg}^{max} and $m_{dg,\omega}^{DG}$ can be calculated according to (34) and (35). Equations (2)–(5) can be replaced by (36)–(39), respectively. Value of V_i^{est} can be calculated according to (40). The relationship between directional power and the pieces of active and reactive power ($\Delta p_{ij,\omega}, \Delta q_{ij,\omega}$) flowing in lines as well as their upper bounds are determined in (41)–(44), while the value of Δp_{ij}^{max} is presented in (45). Finally, (7) and (8) are substituted by (46) and (47), respectively.

$$min\left(\sum_t \Delta_t \mathbb{C}_t^{Main} p_t^{Main} + \sum_{dg}\sum_t \mathbb{C}_{dg}^{a}\varrho_{dg,t}^{DG} + \Delta_t p_{dg,t}^{DG}\mathbb{C}_{dg}^{b} + \Delta_t{}^2\mathbb{C}_{dg}^{c}\left(M_{dg,\omega}^{DG}\Delta p_{dg,t,\omega}^{DG}\right)\right) \tag{31}$$

$$P_{dg,t}^{DG} = \sum_{\omega}\Delta p_{dg,t,\omega}^{DG};\forall dg,t \tag{32}$$

$$\Delta p_{dg,t,\omega}^{DG} \leq \Delta P_{dg}^{max};\ \forall dg,t,\omega \tag{33}$$

$$\Delta P_{dg}^{max} = \left(P_{dg}^{max} - P_{dg}^{min}\right)/\varpi\,;\ \forall dg \tag{34}$$

$$M_{dg,\omega}^{DG} = (2\omega - 1)\Delta P_{dg}^{max};\forall dg,\omega \tag{35}$$

$$\sum_{ki|ki\in L} p_{ki,t} - \sum_{ij|ij\in L}\left(p_{ij,t} + R_{ij} i_{ij,t}^{sqr}\right) + \sum_{i|b_{sub=i}} p_{i,t}^{Main} + \sum_{dg|b_{dg}=i} p_{dg,t}^{DG} + \sum_{pv|b_{pv}=i} p_{pv,t}^{PV} = L_{i,t}^{P} + \sum_{bs|b_{bs}=i} p_{bs,t}^{BS};\ \forall i,t \tag{36}$$

$$\sum_{ki|ki\in L} q_{ki,t} - \sum_{ij|ij\in L}\left(q_{ij,t} + X_{ij} i_{ij,t}^{sqr}\right) + \sum_{i|i=b_{sub}} q_{i,t}^{Main} + \sum_{dg|b_{dg}=i} q_{dg,t}^{DG} = L_{i,t}^{Q};\ \forall i,t \tag{37}$$

$$v_{i,t}^{sqr} - v_{j,t}^{sqr} = 2\left(R_{ij}p_{ij,t} + X_{ij}q_{ij,t}\right) + Z_{ij}^{2} i_{ij,t}^{sqr} + \Gamma_{ij,t};\ \forall ij|ij\in L,t \tag{38}$$

$$V_i^{est} i_{ij}^{sqr} = \sum_{\omega} M_{ij,\omega}^{pq}\left(\Delta p_{ij,\omega} + \Delta q_{ij,\omega}\right);\forall ij \tag{39}$$

$$V_i^{est} = (V_{max}^2 + V_{min}^2)/2\,;\ \forall i \tag{40}$$

$$\sum_{\omega}(\Delta p_{ij,\omega}) = p_{ij}^{+} + p_{ij}^{-};\ \forall ij|ij\in L \tag{41}$$

$$\sum_{\omega}(\Delta q_{ij,\omega}) = q_{ij}^{+} + q_{ij}^{-};\ \forall ij|ij\in L \tag{42}$$

$$\Delta p_{ij,\omega} \le \Delta P_{ij}^{max};\ \forall ij|ij\in L,\omega \tag{43}$$

$$\Delta q_{ij,\omega} \le \Delta Q_{ij}^{max};\ \forall ij|ij\in L,\omega \tag{44}$$

$$\Delta P_{ij}^{max} = \Delta Q_{ij}^{max} = (V_{max}I_{max})/\varpi\,;\ \forall ij|ij\in L \tag{45}$$

$$(V^{min})^2 \le v_{i,t}^{sqr} \le (V^{max})^2;\ \forall i,t \tag{46}$$

$$0 \le i_{ij,t}^{sqr} \le \left(I_{ij}^{max}\right)^2\left(y_{ij}^{+} + y_{ij}^{-}\right);\ \forall ij|ij\in L,t \tag{47}$$

III. RESULTS AND FINDINGS

The profile of electricity price and PV generation are illustrated in Fig. 1 [13]. In addition, the profile of active and reactive power demand is shown in Fig. 2 as presented in [18]. To evaluate the presented MILP models, a modified IEEE 33-bus network [19] integrated by four 600 kW PV units, a 400 kW DG unit, and a 500 kVA battery is considered. The 33-bus grid-connected RMG is depicted in Fig. 3. The proposed MILP models have been implemented in GAMS [20] and solved by CPLEX [21], using a computer with an Intel i7-6500U processor and 8 GB of RAM.

A. *Case I: Optimal operation of MG without reconfiguration*

In this case the total operation cost of MG is obtained \$3368.56. The scheduling of the DG unit and energy level of the battery is depicted in Fig. 4. Moreover, the active and reactive power imported from the main grid is illustrated in Fig. 5. Voltage profiles are depicted in Fig. 6. It is worth mentioning the total power loss is achieved 464.34 kWh for the whole time interval.

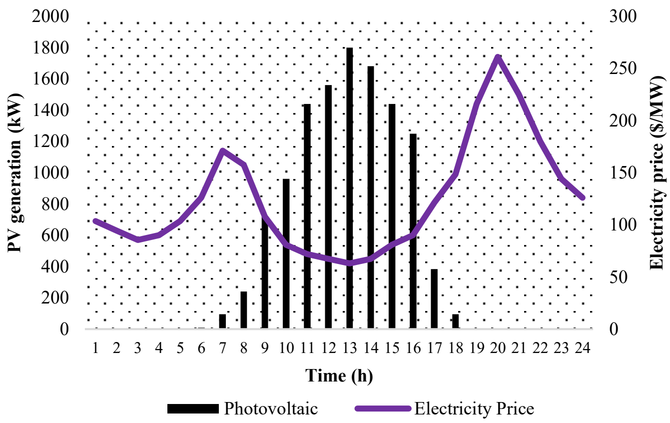

Fig. 1. Expected PV generation and electricity prices

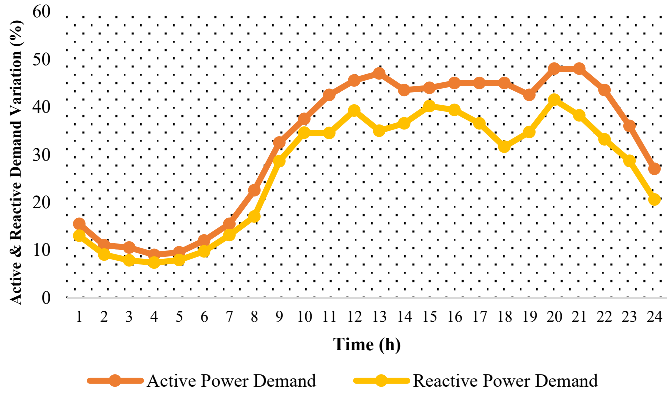

Fig. 2. Active and reactive power demand

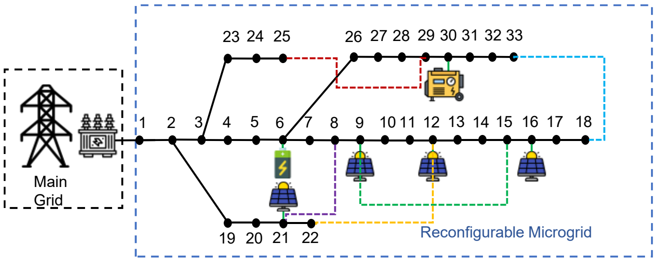

Fig. 3. Schematic diagram of reconfigurable microgrid

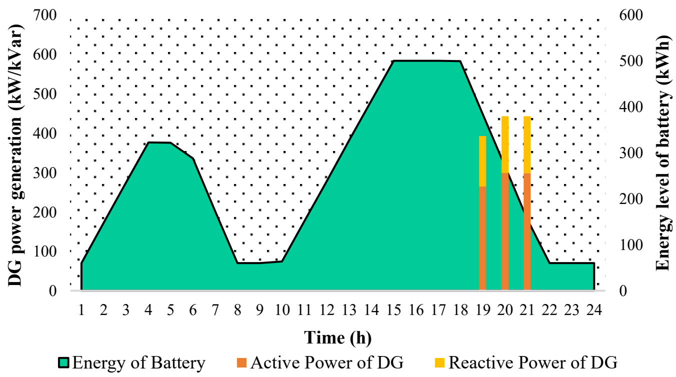

Fig. 4. Scheduling of DG and energy level of battery in Case I

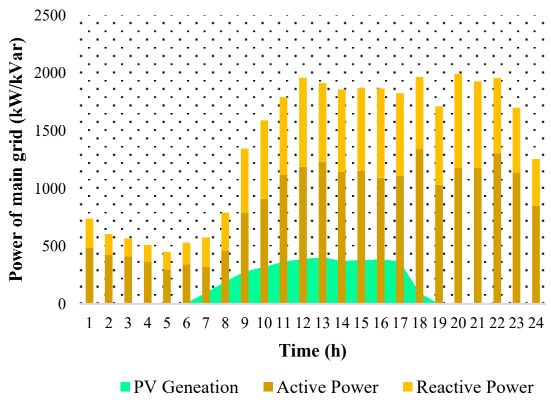

Fig. 5. Power imported from the main grid to RMG in Case I

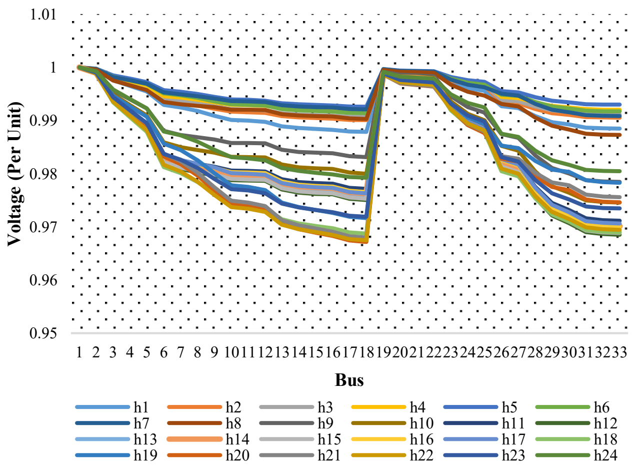

Fig. 6. Voltage profiles in Case I

B. *Case II: Optimal operation of MG with reconfiguration*

In this case, the optimal scheduling of the MG is determined, while hourly reconfiguration is considered. Thus, the number of discrete variables is 1848 consisting of 1776 binary variables linked to status of switches of 37 lines, 48 binary variables related to charging/discharging of the battery, and 24 binary variables are associated with commitment of the DG unit. The computation time for 2% relative gap (i.e., optcr=0.02 [21]) is 16237 seconds deploying (28)–(30) to enforce the radiality. In this case the total operation cost of MG is obtained $2376.695. The scheduling of the DG unit and energy level of the battery is depicted in Fig. 7. It can be notice that during the second peak electricity price (i.e., $t = 19, 20, 21, 22$) the DG unit generates power so as to less power needed to be purchased from the main grid, while battery also discharges up to its lower bound limit. Moreover, the active and reactive power imported from the main grid is illustrated in Fig. 7. Voltage profiles are depicted in Fig. 9 . It is worth mentioning the total power loss is achieved 275.104 kWh for the whole time interval. Therefore, the results show that considering reconfigurability not only reduce the total cost but also reduce the PL and renewable curtailment of RMG. However, the computational time is substantially high for a day-ahead scheduling of RMGs. It is noteworthy hat, the problem is intractable using (27) and (28) to impose radiality as it cannot reach the solution before 86400 seconds (i.e., 24 hours). As a result, the computational time can depend significantly on the method to impose the radiality in RMGs.

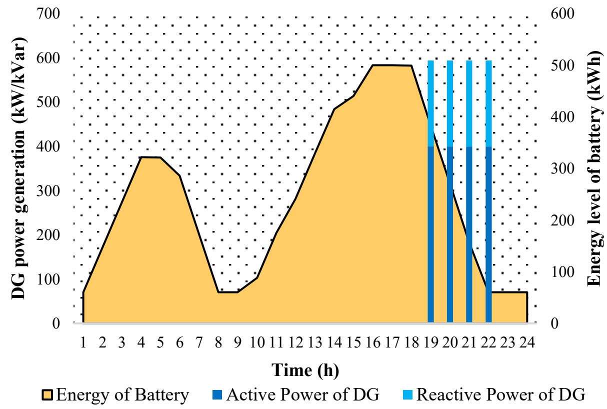

Fig. 7. Scheduling of DG and energy level of battery in Case II

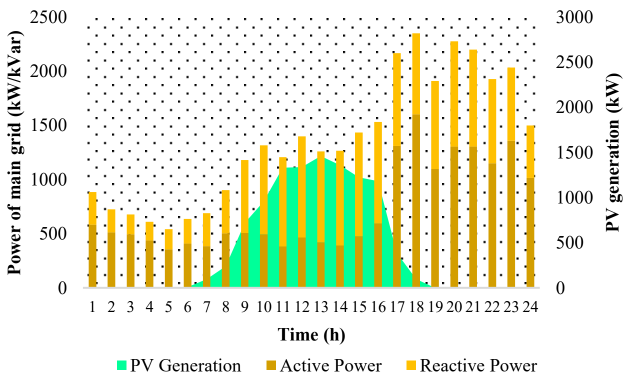

Fig. 8. Power imported from the main grid to RMG in Case II

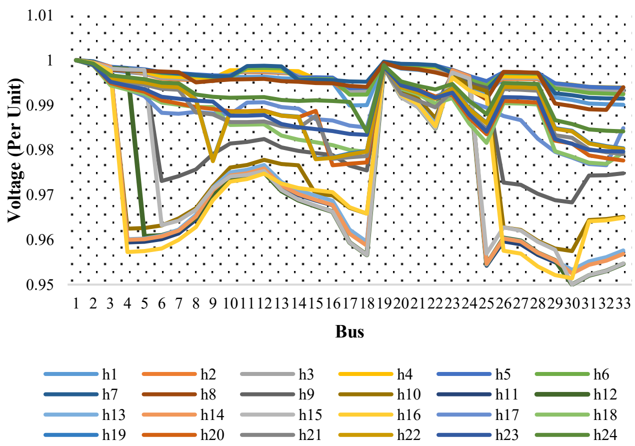

Fig. 9. Voltage profiles in Case II

IV. Conclusion

Reconfiguration can be beneficial for microgrids (MGs) as it enables them to address power quality issues, such as voltage rise or drop within the system. Furthermore, contingencies and renewable energy curtailment can be effectively mitigated by altering the configuration of MGs and redirecting power flow through the systems. Consequently, this research initially developed a nonlinear model for a photovoltaic-integrated reconfigurable microgrid (RMG). It was demonstrated that due to the large number of binary variables linked to the status of switches, even the linearized model for day-ahead scheduling of RMGs proves to be computationally inefficient. Moreover, our investigation into the effects of different radiality methods on computational times provided valuable insights, highlighting the importance of algorithmic efficiency without compromising on solution quality. This investigation underscored the critical role of reconfiguration in optimizing the performance of renewable-based RMGs, while also emphasizing the significant computational considerations necessary for the effective design and implementation of such advanced systems.

This research indicated that even a modest-sized RMG, with a handful of photovoltaic systems, a single distributed generation unit, and a battery, can experience significant computational burden. When uncertainty is factored in, for instance through stochastic programming and scenario generation, the complexity exacerbates as the count of variables and constraints grows substantially. This underscores the need for additional investigation into managing uncertainty and the computational load in RMGs, particularly in cases where metaheuristic optimization is not an option and the optimality of solutions is crucial.

REFERENCES

[1] M.-A. Dupré la Tour, "Photovoltaic and wind energy potential in Europe – A systematic review," Renew. Sustain. Energy Rev., vol. 179, p. 113189, 2023, doi: https://doi.org/10.1016/j.rser.2023.113189.

[2] S. Tajjour and S. Singh Chandel, "A comprehensive review on sustainable energy management systems for optimal operation of future-generation of solar microgrids," Sustain. Energy Technol. Assessments, vol. 58, p. 103377, 2023, doi: https://doi.org/10.1016/j.seta.2023.103377.

[3] S. F. Zandrazavi, C. P. Guzman, A. T. Pozos, J. Quiros-Tortos, and J. F. Franco, "Stochastic multi-objective optimal energy management of grid-connected unbalanced microgrids with renewable energy generation and plug-in electric vehicles," Energy, vol. 241, p. 122884, 2022.

[4] J. M. Home-Ortiz, L. H. Macedo, R. Vargas, R. Romero, J. R. S. Mantovani, and J. P. S. Catalao, "Increasing RES hosting capacity in distribution networks through closed-loop reconfiguration and Volt/VAr control," IEEE Trans. Ind. Appl., vol. 58, no. 4, pp. 4424–4435, 2022.

[5] A. K. Barnwal, L. K. Yadav, and M. K. Verma, "A multi-objective approach for voltage stability enhancement and loss reduction under PQV and P buses through reconfiguration and distributed generation allocation," IEEE Access, vol. 10, pp. 16609–16623, 2022.

[6] F. Yaprakdal, M. Baysal, and A. Anvari-Moghaddam, "Optimal operational scheduling of reconfigurable microgrids in presence of renewable energy sources," Energies, vol. 12, no. 10, p. 1858, 2019.

[7] M. Hemmati, B. Mohammadi-Ivatloo, M. Abapour, and A. Anvari-Moghaddam, "Day-ahead profit-based reconfigurable microgrid scheduling considering uncertain renewable generation and load demand in the presence of energy storage," J. Energy Storage, vol. 28, p. 101161, 2020.

[8] M. Hemmati, B. Mohammadi-Ivatloo, S. Ghasemzadeh, and E. Reihani, "Risk-based optimal scheduling of reconfigurable smart renewable energy based microgrids," Int. J. Electr. Power Energy Syst., vol. 101, pp. 415–428, 2018.

[9] A. Kavousi-Fard and A. Khodaei, "Efficient integration of plug-in electric vehicles via reconfigurable microgrids," Energy, vol. 111, pp. 653–663, 2016, doi: https://doi.org/10.1016/j.energy.2016.06.018.

[10] M. Sedighizadeh, G. Shaghaghi-shahr, M. Esmaili, and M. R. Aghamohammadi, "Optimal distribution feeder reconfiguration and generation scheduling for microgrid day-ahead operation in the presence of electric vehicles considering uncertainties," J. Energy Storage, vol. 21, pp. 58–71, 2019, doi: https://doi.org/10.1016/j.est.2018.11.009.

[11] S. F. Zandrazavi, A. Tabares Pozos, and J. F. Franco, "Data Clustering Method for Probabilistic Power Flow in Microgrids," in Handbook of Smart Energy Systems, Springer, 2023, pp. 1133–1154.

[12] IBM, "IBM ILOG CPLEX Optimization Studio." [Online]. Available: https://www.gams.com/products/gams/gams-language/

[13] S. F. Zandrazavi and M. Shafie-Khah, "Resilient energy management of networked microgrids and renewable energy resource," in Future Modern Distribution Networks Resilience, Elsevier, 2024, pp. 279–302.

[14] M. Ebrahimi, M. Ebrahimi, A. Fallah, M. Shafie-Khah, and H. Laaksonen, "An iterative auction-based method for multi energy trading in a microgrid considering renewable energy uncertainties," Electr. Power Syst. Res., vol. 232, p. 110381, 2024, doi: https://doi.org/10.1016/j.epsr.2024.110381.

[15] M. Lavorato, J. F. Franco, M. J. Rider, and R. Romero, "Imposing Radiality Constraints in Distribution System Optimization Problems," IEEE Trans. Power Syst., vol. 27, no. 1, pp. 172–180, 2012, doi: 10.1109/TPWRS.2011.2161349.

[16] R. A. Jabr, R. Singh, and B. C. Pal, "Minimum Loss Network Reconfiguration Using Mixed-Integer Convex Programming," IEEE Trans. Power Syst., vol. 27, no. 2, pp. 1106–1115, 2012, doi: 10.1109/TPWRS.2011.2180406.

[17] S. F. Zandrazavi, A. T. Pozos, J. F. Franco, and M. Shafie-khah, "Planning the operation and expansion of power distribution systems considering electric vehicles (smart charging)," in Advanced Technologies in Electric Vehicles, Elsevier, 2024, pp. 259–277.

[18] O. D. Montoya, A. Garces, and W. Gil-González, "Minimization of the distribution operating costs with D-STATCOMS: A mixed-integer conic model," Electr. Power Syst. Res., vol. 212, p. 108346, 2022.

[19] Matpower, "Power flow data for 33 bus distribution system from Baran & Wu."

[20] G. D. Corporation, "GAMS - The Modeling Language." [Online]. Available: https://www.gams.com/products/gams/gams-language/

[21] G. D. Corporation, "GAMS CPLEX Solver Documentation." [Online]. Available: https://www.gams.com/latest/docs/S_CPLEX.html